

RELAMINARIZATION OF TURBULENT CHANNEL FLOW USING TRAVELING WAVE-LIKE WALL DEFORMATION

Rio Nakanishi, Koji Fukagata, Hiroya Mamori

Department of Mechanical Engineering
Keio University

Hiyoshi 3-14-1, Kohoku-ku, Yokohama 223-8522, Japan
nakanishi@fukagata.mech.keio.ac.jp

ABSTRACT

Effect of traveling wave-like wall deformation (i.e. peristalsis) in a fully developed turbulent channel flow is investigated by means of direct numerical simulation. We not only demonstrate that the friction drag is reduced by wave-like wall deformation traveling toward the downstream direction, but also show that the turbulence is completely killed (viz. the flow is re-laminarized) under some sets of parameters. It is also found that at higher amplitude of actuation the re-laminarized flow is unstable and exhibits a periodic cycle between high and low drag.

Introduction

Drag reduction in wall-bounded turbulent flow is of great importance for mitigating environmental impact through the efficient utilization of energy. The large friction drag in turbulent flows on a solid wall, as compared to that in laminar flows, is attributed to the vortical structure in the region near the wall (Robinson, 1991). Passive devices such as riblets (Walsh, 1983) and structured roughness (Sirovich and Karlsson, 1997) are known to have friction drag reduction effect on the order of 10% by interacting with these vortical structure. In order to gain larger effects, recent efforts have been made to actively suppress these structures to reduce the friction drag in wall-turbulence, e.g. by predetermined spanwise traveling wave (Du and Karniadakis, 2000) and feedback control using actuation from the wall (Kim, 2003; Kasagi *et al.*, 2009).

Mathematically, the friction drag coefficient C_f of a fully-developed turbulent flow in a two-dimensional channel is expressed by using a weighted integration of the Reynolds shear stress ($-\overline{u'v'}$), i.e. (Fukagata *et al.*, 2002)

$$C_f = \frac{12}{Re_b} + 24 \int_0^1 (1-y)(-\overline{u'v'})dy, \quad (1)$$

where $Re_b = 2U_b h/\nu$ (with U_b , h , and ν being the bulk-mean velocity, the channel half-width, and the kinematic viscosity, respectively) is the bulk Reynolds number and y denotes the non-dimensionalized distance from the wall. This identity equation not only suggests that the friction drag can be reduced by reducing the Reynolds shear stress, especially in the

region near the wall, but also implies that the drag can reach a sub-laminar level if the second term can be made largely negative.

Based on this implication, Min *et al.*(2006) proposed a novel predetermined control method using traveling wave-like blowing and suction from the walls. They showed by means of numerical simulation that the blowing and suction traveling toward the upstream direction (hereafter referred to as the upstream traveling wave) significantly reduce the near-wall Reynolds shear stress. They also demonstrated that under some sets of parameters the drag can be reduced to a sub-laminar level by making the near-wall Reynolds shear stress largely negative.

Min *et al.*(2006)'s control is attractive in the sense that it does not require massive sensors and is much simpler than the advanced feedback control methods (Kim, 2003; Kasagi *et al.*, 2009). Therefore, several follow-up studies have been made to investigate the stability (Lee *et al.*, 2008; Moarref & Jovanović, 2010; Lieu *et al.*, 2010) and scaling (Mamori *et al.*, 2010) of this control. However, in terms of fabrication of actual devices, the traveling wave-like blowing and suction is still complicated. One possibility toward the practical application is to replace it by a traveling wave-like deforming surface, which may be driven by a smaller number of actuators.

The primary mechanism of drag reduction by traveling wave-like blowing and suction is considered to be *pumping* from the wall. Hœpffner & Fukagata (2009) found in their numerical simulations in the absence of base flow that the traveling wave-like deforming wall (more generally known by the term “peristalsis”) has the pumping effect in the same direction as the wave travels, while the traveling wave-like blowing and suction has the pumping effect in the opposite direction. This difference suggests that the drag reduction using the deformable wall is expected not by the upstream traveling wave but by the downstream traveling wave (note that very recent studies (Moarref & Jovanović, 2010; Lieu *et al.*, 2010) show that high-speed downstream traveling wave-like blowing and suction also re-laminarizes the flow: in that case, the primary mechanism responsible for the drag reduction may not be the pumping from the wall but stabilization).

Drag reduction effect by such downstream traveling

wave-like wall deformation was also experimentally found almost 40 years ago. Taneda and Tomonari (1973) conducted an experiment on a spatially developing boundary layer on a plate waving like the swimming motion of fish. They observed laminarization effect by a downstream traveling wave at a wavespeed much faster than the uniform flow. They also found that the waving plate under some conditions makes the boundary layer cyclically laminar and turbulent. Shen *et al.* (2003) investigated a flow around a similar wavy wall by means of direct numerical simulation (DNS). They showed that the total drag as well as the net power can be reduced by downstream traveling wave. Both studies deal with wavy walls with relatively large amplitude and discuss drag reduction as compared to the case of stationary wave. From the viewpoint of drag reduction control, however, it is important to clarify how the drag is reduced as compared to that of a turbulent flow on a flat surface.

In the present study, we investigate by means of DNS the drag reduction effect of the traveling wave-like deforming wall in a turbulent channel flow. We not only confirm that the drag is reduced by the downstream traveling wave, but also demonstrate that the flow is re-laminarized under some sets of parameters. Indeed, as has been proved mathematically (Bewley, 2009; Fukagata *et al.*, 2009), re-laminarization is the ultimate goal of drag reduction control in terms of energy saving.

Direct Numerical simulation

The DNS code is based on the channel flow code of Fukagata *et al.* (2006) adapted to boundary fitted coordinates. In order to express the wall deformation, the Cartesian coordinates u_i are transformed into ξ_i following Kang & Choi (2000). The traveling wave-like deformation of wall is given as the boundary condition. At the lower wall ($\xi_2 = 0$), for instance, it reads,

$$u_1 = u_3 = 0, u_2 = \frac{\partial \eta_d}{\partial t} = a \cos(k(x - ct)), \quad (2)$$

where a , k , and c denote the velocity amplitude, the wave-number, and the phase-speed of wall deformation, respectively. The upper wall deforms in-phase with the lower wall (i.e. varicose mode). The schematic of traveling wave-like wall deformation is shown in Fig. 1. The displacement of lower and upper wall, η_d and η_u , is obtained by integrating Eq. (2) in time, i.e.

$$\eta_d = -\frac{a}{kc} \sin(k(x - ct)), \eta_u = \frac{a}{kc} \sin(k(x - ct)). \quad (3)$$

The size of computational box is $4\pi \times 2 \times 3.5$ in the streamwise (ξ_1), wall-normal (ξ_2), and spanwise (ξ_3) directions and the corresponding number of computational cells is $256 \times 96 \times 128$. The time step is set to be $\Delta t = 0.01$ in most cases, while $\Delta t = 0.005$ for $k \geq 3$ or $a \geq 0.15$ cases in order to sufficiently resolve the temporal change of boundary condition and the near-wall flow induced thereby. Hereafter, all the variables are non-dimensionalized by using the channel half-width h and twice the bulk-mean velocity $2U_b$. All DNS is performed under a constant flow rate. The bulk Reynolds number is set at

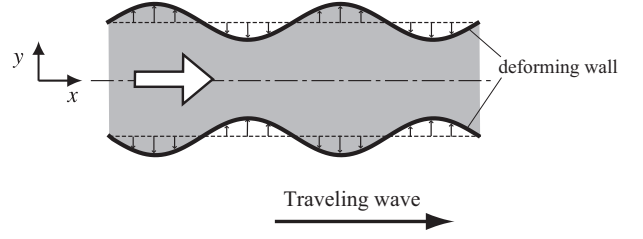


Figure 1. Schematic of a channel with traveling-wave like wall deformation.

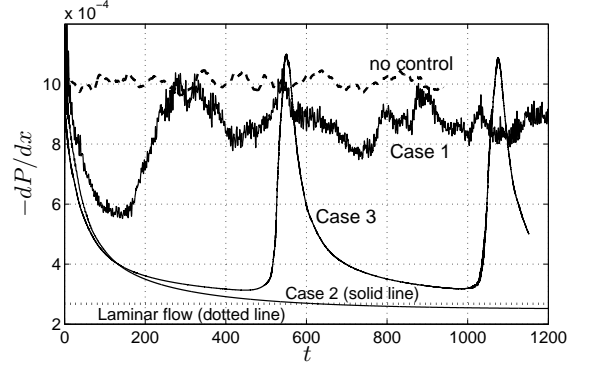


Figure 2. Time trace of mean pressure gradient $-dP/dx$: Case 1 ($a = 0.1, c = 1, k = 2$), ordinary drag reduction; Case 2 ($a = 0.1, c = 1, k = 4$), stable re-laminarization; Case 3 ($a = 0.2, c = 3, k = 4$), unstable re-laminarization.

$Re_b = 2U_b h / \nu = 5600$, corresponding to the friction Reynolds number of $Re_\tau \simeq 180$ in the uncontrolled (i.e. solid wall) case.

Results and Discussion

Drag reduction effects

The DNS runs with different sets of parameters a , k , and c revealed that as a rule the drag is decreased in the cases of $c > 0$ (i.e. downstream traveling waves) and increased for $c < 0$ (i.e. upstream traveling waves). Figure 2 shows the time trace of mean pressure gradient $-dP/dx$ in typical cases of drag reduction. Case 1 is an example of ordinary drag reduction, in which the drag is reduced but the flow remains turbulent. Case 2 exemplifies the case of re-laminarization: the turbulent fluctuations completely vanish and $-dP/dx$ converges close to the value of laminar channel flow. At the steady state, the pressure gradient is slightly lower than the laminar value, which indicates that a small amount of pumping is replaced by the peristaltic pumping. Although the peristaltic pumping is about twice expensive (i.e. power-consuming) than the external pressure gradient (Höpfner & Fukagata, 2009), the present result shows that the contribution of peristaltic pumping is considerably small and thus the net energy saving rate is close to the drag reduction rate (about 70%). Case 3 is a case of unsteady re-laminarization: $-dP/dx$ decreases toward the laminar value but rapidly increases again to the uncontrolled value.

Figure 3 summarizes the control effect under different

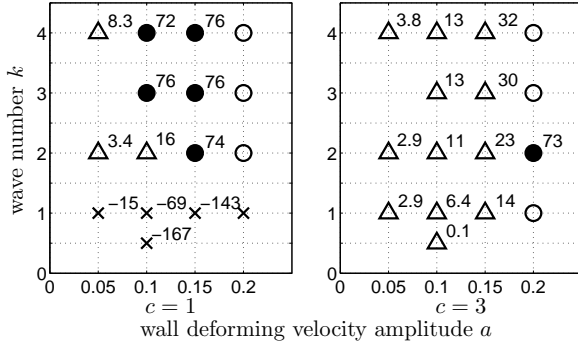


Figure 3. Drag change by the traveling wave-like deforming wall: \times , drag increase; \triangle , ordinary drag reduction; \bullet , stable re-laminarization; \circ , unstable re-laminarization. The value noted together with the symbols (except for the unsteady re-laminarization cases) is the drag reduction rate R_D defined by Eq. (4)

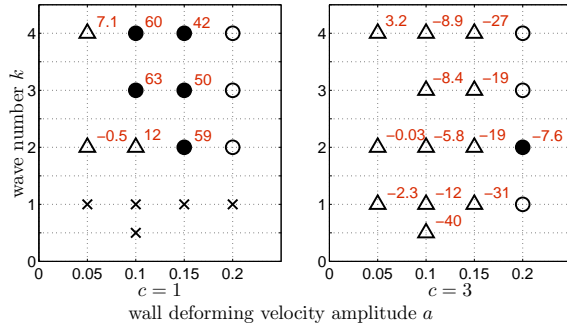


Figure 4. Net power saving effect by the traveling wave-like deforming wall: symbols are the same as those in Fig. 3. The value noted together with the symbols (except for the drag increasing cases and the unsteady re-laminarization cases) is the net power saving rate S defined by Eq. (5)

sets of parameters. The drag reduction rate R_D noted together with the symbols is defined as

$$R_D = \frac{\mathcal{P}_0 - \mathcal{P}}{\mathcal{P}_0} \times 100 [\%], \quad (4)$$

where $\mathcal{P} = -\overline{dP/dx}$ denotes the mean pressure gradient and \mathcal{P}_0 is that in the uncontrolled flow. The map indicates that for both phase-speeds ($c = 1$ and $c = 3$) the flow is re-laminarized by actuation of relatively high wave-number (k) and amplitude (a), but becomes unstable again if the amplitude is further increased.

Figure 4 shows the net power saving effect by wall deformation. The net power saving rate S is defined as

$$S = \frac{W_{p0} - (W_p + W_a)}{W_{p0}} \times 100 [\%], \quad (5)$$

where W_p and W_a are the pumping power and power required for wall deformation, respectively; W_{p0} denotes the pumping

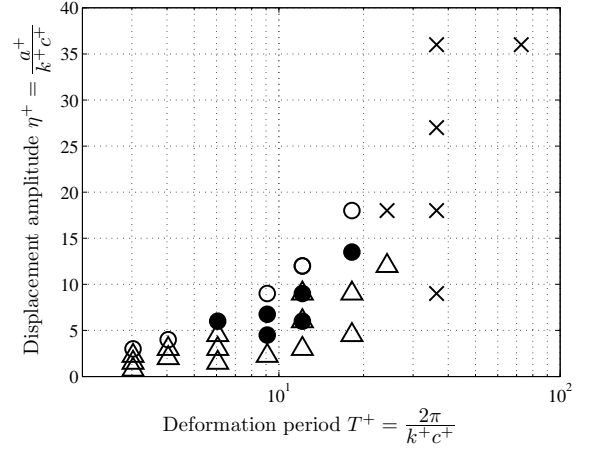


Figure 5. Response of the flow to the traveling wave-like deforming wall: symbols are the same as those in Fig. 3.

power of the uncontrolled flow. It can be noticed that the net power is reduced in the cases of $c = 1$ (left of figure 4). The net power saving effect is noticeable in the re-laminarization cases: the maximum net power saving rate is 63 %. In the cases of $c = 3$ (right of figure 4), however, the net power is not saved even in the re-laminarization cases. This means that faster traveling wave need larger power for actuation than the pumping power reduced.

Figure 5 summarizes the control effect under different sets of parameters. The horizontal axis is the deformation period and the vertical axis is the displacement amplitude, both in wall units. Roughly speaking, the drag decreases with $T^+ < 20$ and increases with $T^+ > 30$. The drag is nearly unchanged at $20 < T^+ < 30$. Also noticed is that re-laminarization is achieved when the displacement amplitude $5 < \eta^+ < 15$ and the flow is unstable when $\eta^+ > 15$. This is different from Taneda and Tomonari (1973)'s result, where the displacement achieving the drag reduction is on the order of boundary layer thickness.

Instantaneous flow field

Figure 6 illustrates four instantaneous flow fields during the process of re-laminarization in the case of $(a, k, c) = (0.1, 4, 1)$. For each time instant, the mean velocity profiles and the contour of Reynolds shear stress $-\overline{u'v'}$ in an $x - y$ plane are shown in the left figure; the cross-sectional velocity vectors and the streamwise velocity contour are shown in the right figure. In the uncontrolled flow (Fig. 6(a)), we observe a flattened mean velocity profile (left) and streaky and vortical structures (right), which are typical to turbulent channel flows. As the time goes (Figs. 6(b)-(c)), an organized Reynolds shear stress distribution is formed near the wall due to the actuation, the velocity profile becomes less flattened thereby (left), and the streaky and vortical structures are weakened (right). Finally, after a sufficiently long time (Fig. 6(d)), the velocity profile becomes similar to the Poiseuille profile (left) and the streaky and vortical structures completely vanish (right).

In the re-laminarized state, the Reynolds shear stress distribution has a cellular structure (Fig. 6(d), left) akin to that observed in the laminar flow with traveling wave-like blow-

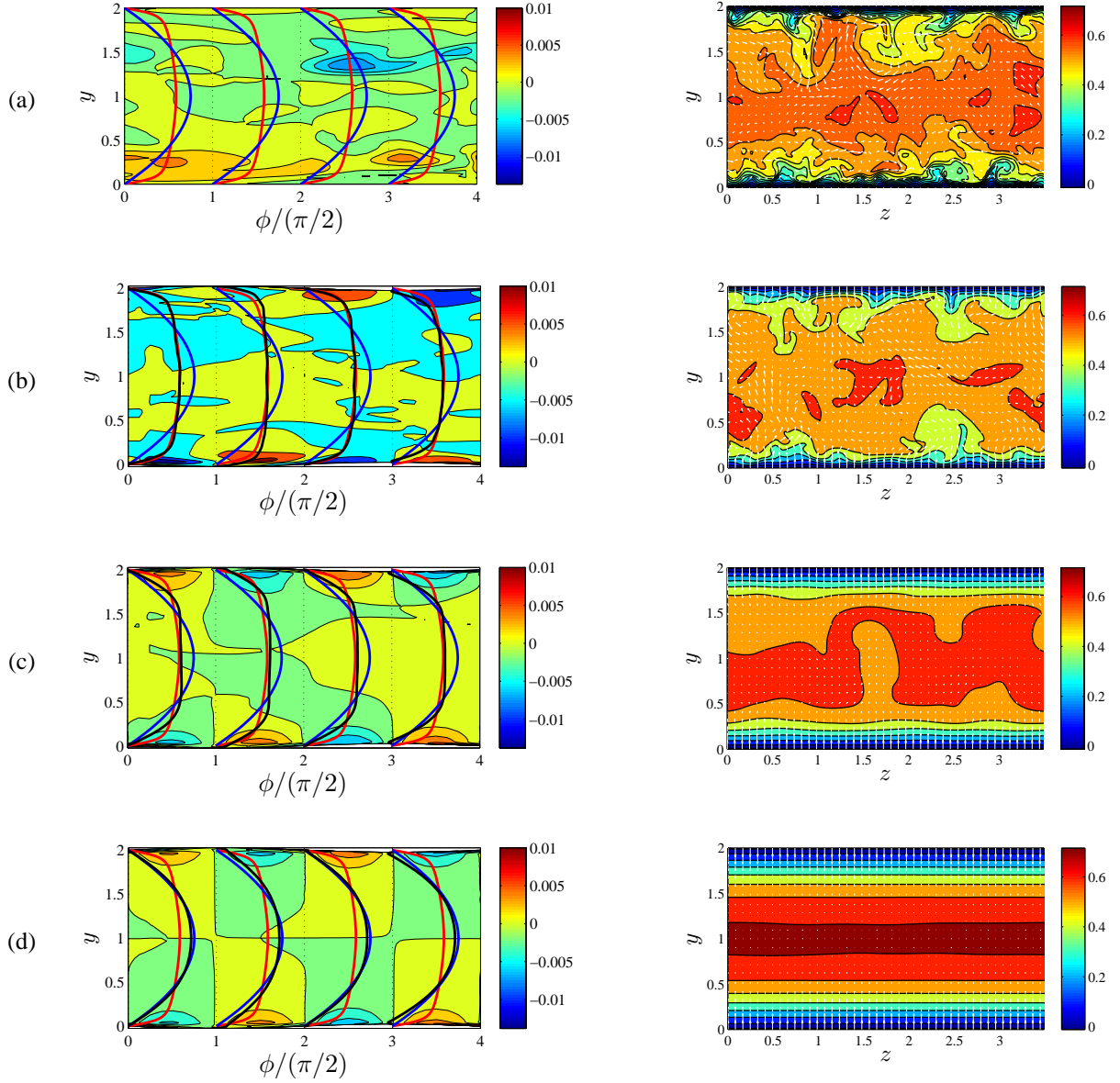


Figure 6. Instantaneous flow fields during the process of re-laminarization (the case of $a = 0.1$, $c = 1$, and $k = 4$): (a) uncontrolled; (b) $t = 15.7$; (c) $t = 156.0$; (d) $t = 628.3$. Figures in the left column shows the streamwise velocity and Reynolds shear stress in the $x - y$ plane: black line, streamwise velocity averaged at each phase ($\phi = 0, \pi/2, \pi, 3\pi/2$); red line, uncontrolled turbulent profile; blue line, laminar Poiseuille profile; color contour, Reynolds shear stress $-\overline{u'v'}$. Figures in the right column shows the velocity field in the $z - y$ plane at $\phi = 0$, at which the deformation velocity is maximum: vector, wall-normal and spanwise velocity; color contour, streamwise velocity.

ing/suction (Mamori *et al.*, 2010). The peak of $-\overline{u'v'}$ is located close to the wall due to the wall-normal velocity induced by the wall deformation, whereas $-\overline{u'v'}$ is found to be nearly zero in the region far from the wall. Although the mean velocity profile is close to the Poiseuille profile, a small amount of reverse flow is also observed near the wall in the phases of $0 \leq \phi/(\pi/2) \leq 0.1$ and $2.5 \leq \phi/(\pi/2) \leq 4$. This is due to the wall deformation, which carries the fluid particles back and forth so that they draw ℓ -shaped drifting tracks (Höpfner & Fukagata, 2009).

In the unsteady re-laminarization cases, the process of re-laminarization is almost the same as that in the steady re-laminarization cases. Figure 7 shows the evolution of flow in which the re-laminarized flow (7(a)) is destabilized (7(b)-(d)) and stabilized again (7(e)-(f)). When the pressure gradient begins to increase, the low-speed fluid is ejected from the near-wall region and vortical structure appears (Fig. 7(b), right.) Similar phenomena are observed at different places (Fig. 7(c), right), accompanying the development of Reynolds shear stress. Accordingly, the mean streamwise velocity pro-

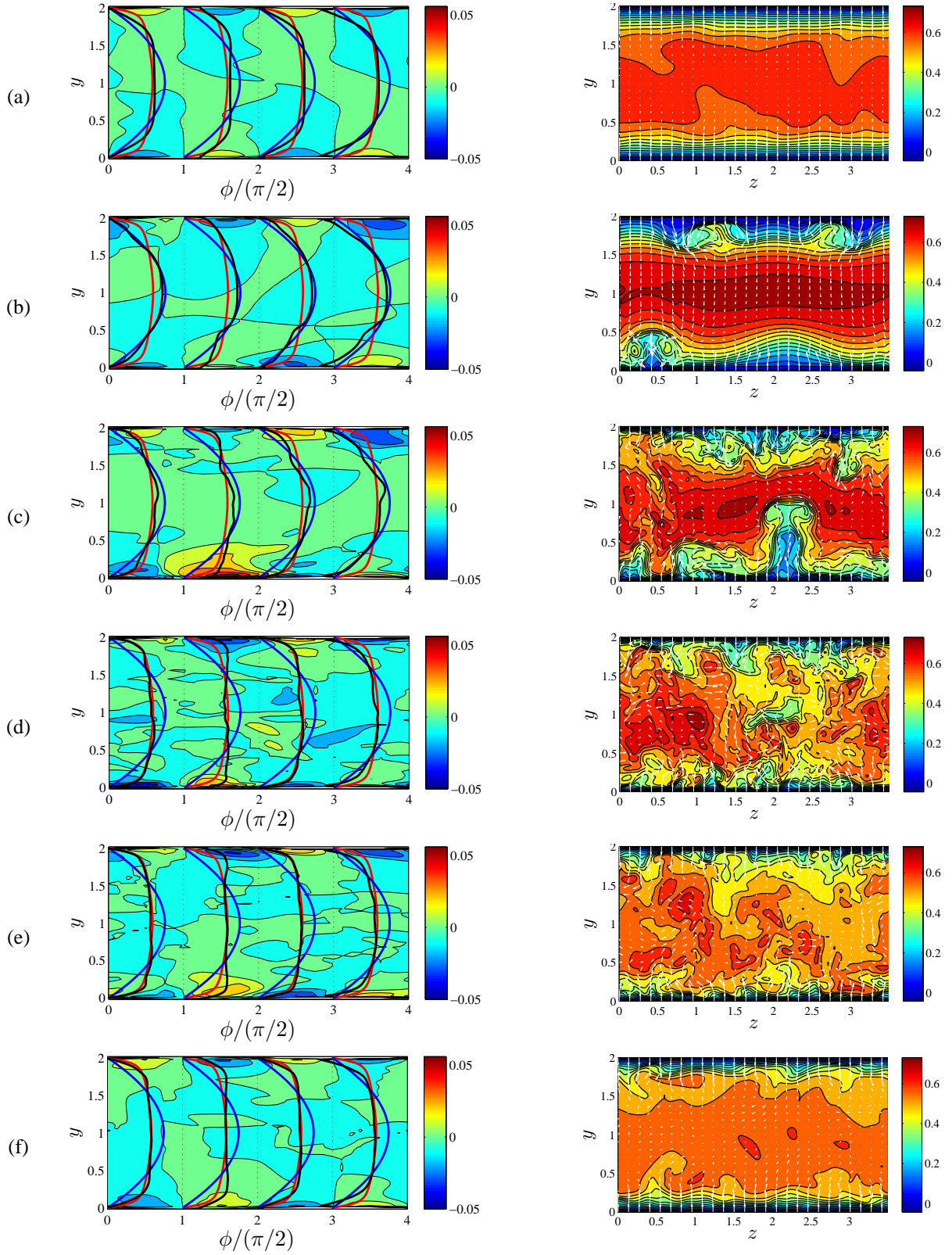


Figure 7. Instantaneous flow fields during the process that re-laminarized flow return to turbulence rapidly (the case of $a = 0.2$, $c = 3$, and $k = 4$): (a) $t = 156.0$; (b) $t = 518.4$; (c) $t = 534.1$; (d) $t = 550.0$; (e) $t = 565.5$; (f) $t = 612.6$. The contents are same as Fig. 6

file is distorted (left). At the time when the mean pressure gradient is maximized (Fig. 7(d)), low-speed region, vortices, and Reynolds shear stress spread in whole channel. The Reynolds shear stress distribution and the mean velocity profile looks similar to those of the uncontrolled flow (Fig. 6(a)) After that time, the low-speed region and the vortices weakened (Fig. 7(e)-(f), right) and the flow is re-laminarized again.

As compared to the steady re-laminarized case, Fig. 6(d), the reverse flow near the wall in Fig. 7(a) is stronger due to the higher amplitude of wall deformation. This stronger reverse flow makes an inflection point in the mean streamwise velocity profile to cause the instability as observed in Fig. 2.

Conclusions

We demonstrated by means of DNS that the downstream traveling wave-like wall deformation significantly reduces the drag. The primary drag reduction mechanism can be explained by the pumping effect in the same direction as the wave (Høpfner & Fukagata, 2009). In the present study, we observe that under several sets of parameters this control can also re-laminarize the low Reynolds number turbulent channel flow. Although similar observation has been made in previous studies, e.g., Taneda and Tomonari (1974), a clear distinction with those is that the re-laminarization is achieved with much smaller amplitude of wall deformation, i.e., on the order of viscous sublayer. An interesting phenomenon additionally observed is that with stronger actuation the re-laminarized flow is unstable and exhibits a periodic cycle between high and low drag. The cause and dynamics of this peculiar phenomenon, however, is open for future work.

Acknowledgments

The authors are grateful to Dr. Shinnosuke Obi (Keio University), Dr. Jerome Høpfner (UPMC), Drs. Nobuhide Kasagi and Yosuke Hasegawa (The University of Tokyo), and Dr. Kaoru Iwamoto (Tokyo University of Agriculture and Technology) for fruitful discussions. This work was supported through Grant-in-Aid for Scientific Research (A) (No. 20246036) by Japan Society for the Promotion of Science (JSPS) and Keio University Global COE program of "Center for Education and Research of Symbiotic, Safe and Secure System Design."

REFERENCES

Bewley, T. R. 2009, "A fundamental limit on the balance of power in a transpiration-controlled channel flow", *Journal of Fluid Mechanics*, Vol. 632, pp. 443-446.

Du, Y. and Karniadakis, G. E. 2000, "Suppressing wall turbulence by means of a transverse traveling wave", *Science*, Vol. 288, pp. 1230-1234.

Fukagata, K., Iwamoto, K. and Kasagi, N. 2002, "Contribution of Reynolds stress distribution to the skin friction in wall-bounded flows", *Physics of Fluids*, Vol. 14, L73-L76.

Fukagata, K., Kasagi, N. and Koumoutsakos, P. 2006, "A theoretical prediction of friction drag reduction in turbulent flow by superhydrophobic surfaces", *Physics of Fluids*, Vol. 18, 051703.

Fukagata, K., Sugiyama, K. and Kasagi, N. 2009, "On the lower bound of net driving power in controlled duct flows", *Physica D*, Vol. 238, pp. 1082-1086.

Høpfner, J. and Fukagata, K. 2009, "Pumping or drag reduction?" *Journal Fluid Mechanics*, Vol. 635, pp. 171-187.

Kang, S. and Choi, H. 2000, "Active wall motions for skin-friction drag reduction", *Physics of Fluids*, Vol. 12, pp. 3301-3304.

Kasagi, N., Suzuki, Y. and Fukagata, K. 2009, "Micro-electromechanical systems-based feedback control of turbulence for skin friction reduction", *Annual Review of Fluid Mechanics*, Vol. 41, pp. 231-251.

Kim, J. 2003, "Control of turbulent boundary layers", *Physics of Fluids*, Vol. 15, pp. 1093-1105.

Lee, C., Min, T. and Kim, J. 2008, "Stability of a channel flow subject to wall blowing and suction in the form of a traveling wave", *Physics of Fluids*, Vol. 20, 101513.

Lieu, B., Moarref R. & Jovanović, M. R. 2010, "Controlling the onset of turbulence by streamwise traveling waves. Part 2: Direct numerical simulations", *Journal of Fluid Mechanics*, Vol 663, 100-119.

Mamori, H., Fukagata, K. and Høpfner, J. 2010, "Phase relationship in laminar channel flow controlled by traveling-wave-like blowing or suction", *Physic Review E*, Vol. 81, 046304.

Min, T., Kang, S. M., Speyer, J. L. and Kim, J. 2006, "Sustained sub-laminar drag in a fully developed channel flow", *Journal of Fluid Mechanics*, Vol. 558, pp. 309-318.

Moarref, R. and Jovanović, M. R. 2010, "Controlling the onset of turbulence by streamwise traveling waves. Part 1: Receptivity analysis", *Journal of Fluid Mechanics*, Vol. 664, pp. 70-99.

Robinson, S. K. 1991, "Coherent motions in the turbulent boundary layer", *Annual Review of Fluid Mechanics*, Vol. 23, pp. 601-639.

Shen, L., Zhang, X., Yue, D. K. P. and Triantafyllou, M. S. 2003, "Turbulent flow over a flexible wall undergoing a streamwise traveling wave motion", *Journal of Fluid Mechanics*, Vol. 484, pp. 197-221.

Sirovich, L. and Karlsson, S. 1997, "Turbulent drag reduction by passive mechanisms", *Nature*, Vol. 388, pp. 753-755.

Taneda, S. and Tomonari, Y. 1973, "an Experiment on the Flow around a Waving Plate", *Journal of the Physical Society of Japan*, Vol. 36, pp. 1683-1689.

Walsh, M. J. 1983, "Riblets as a viscous drag reduction technique", *AIAA Journal*, Vo. 21, pp. 485-486.